Thermal conductivity of thermoelectric material β–Cu_2Se: Implications on phonon thermal transport

Sadanandam Namsani, Sushil Auluck, and Jayant K. Singh

Citation: Appl. Phys. Lett. **111**, 163903 (2017);
View online: https://doi.org/10.1063/1.4999405
View Table of Contents: http://aip.scitation.org/toc/apl/111/16
Published by the American Institute of Physics

Thermal conductivity of thermoelectric material β-Cu_2Se: Implications on phonon thermal transport

Sadanandam Namsani,[1] Sushil Auluck,[2] and Jayant K. Singh[1,a)]
[1]*Department of Chemical Engineering, Indian Institute of Technology Kanpur, Kanpur 208016, India*
[2]*CSIR-Network of Institutes for Solar Energy, Materials Physics and Engineering Division, CSIR-National Physical Laboratory, Dr. K. S. Krishnan Road, New Delhi 110012, India*

(Received 8 August 2017; accepted 30 September 2017; published online 17 October 2017)

Thermal transport properties associated with the thermal structure evolution of β-Cu_2Se are studied using density functional theory (DFT) and molecular dynamics (MD) simulations. Thermal conductivity of β-Cu_2Se is calculated over a temperature range of 400–1000 K using reverse non-equilibrium molecular dynamics simulations. The thermal conductivity found through MD simulations decreases monotonically with increasing temperature, which is in line with the reported experimental data and our calculated DFT data. The average phonon mean free path evaluated using the kinetic theory, found to be within the range of 1.0–1.5 Å, decreases with increasing temperature. Furthermore, we have investigated the temperature-dependent heat transport phenomena using phonon density of states, calculated using MD simulations. The phonon modes are found to shift towards the low frequency numbers with increasing temperature, indicating lower heat carrying capacity of the material and in agreement with the computed thermal conductivity. *Published by AIP Publishing.* https://doi.org/10.1063/1.4999405

Thermoelectric technology converts waste heat into useful electricity. Owing to the environmentally friendly nature of thermoelectric technology and its applications in thermal management,[1] many materials have been investigated for different temperature range applications. However, the main impediment of this technology is the low energy conversion efficiency of the commonly used thermoelectric materials.[2] The energy conversion efficiency of a thermoelectric material is governed by the dimensionless thermoelectric figure-of-merit, ZT. The ZT of a material is defined as $ZT = S^2\sigma T/(\kappa_e + \kappa_L)$, where S, σ, T, κ_e, and κ_L are the Seebeck coefficient, electrical conductivity, absolute temperature, electronic thermal conductivity, and lattice thermal conductivity, respectively. In the recent past, many strategies have been proposed to increase the ZT of materials. Crystalline semiconductors with a disordered arrangement of atoms,[1] semiconductors with caged structures,[3,4] and materials with nanoinclusions[5] have been shown to be good thermoelectric materials with high ZT. Cu_2Se is one such material, in which the copper ions show liquid-like behavior. Cu_2Se has gained attention in recent years as a thermoelectric material because of its low thermal conductivity and high thermoelectric figure-of-merit.[6,7] Cu_2Se exhibits two phases: a low-temperature α-phase and a high-temperature β-phase. The α-phase is stable up to about 400 K, whereas the β-phase is stable at higher temperatures. Liu *et al.*[6] have shown that both phases of Cu_2Se display low electrical resistivity ($\boldsymbol{\rho}$) and low Seebeck coefficient (S) over a temperature range of 300–1000 K. Despite the low Seebeck coefficient, they reported a high ZT value of 1.5 at 1000 K for β-phase Cu_2Se. More recently, Gahtori *et al.*[8] induced nano-porosity in Cu_2Se, in the range of nano–mesoscale dimensions, and reported a ZT value of 2.1 at 973 K, an ∼40% increase in the figure-of-merit. A few authors have performed theoretical studies on the high-temperature β-phase using density functional theory (DFT). Mikael *et al.*[9] used various approximations for the exchange correlation energy functions within DFT to study the electronic structure and bulk properties of β-Cu_2Se. Zhang *et al.*[10] performed band structure calculations and reported Cu_2Se as semi-metallic using the modified Becke-Johnson (mBJ) approximation. Recently, Tyagi *et al.*[11] studied the band structure and electric transport coefficient of the high-temperature β-phase of Cu_2Se using DFT. They concluded that Cu_2Se is a good potential p-type thermoelectric material.

From the definition of ZT, it is known that a material should have high S, σ, and T and/or low thermal conductivity to achieve high ZT values. The diverse advanced approaches used in recent years to achieve high ZT values aim to maintain a high power factor ($S^2\sigma$) and/or low thermal conductivity.[12] Among the thermoelectric parameters, the lattice thermal conductivity (κ_L) is the only parameter that is independent of carrier concentration. Thus, the ZT value of a material is very sensitive to the change in κ_L.[13] Hence, the κ_L value of a material plays a key role in determining its ZT. While the κ_L values of various materials have been calculated using equilibrium and non-equilibrium methods,[14] a molecular mechanics-molecular dynamics (MD) investigation has not been carried out for Cu_2Se up to this date. Kim *et al.*[15] reported temperature dependent lattice thermal conductivity values of Cu_2Se using non-equilibrium *ab-initio* molecular dynamics (NEAIMD) simulations. These simulations were performed using limited cell volumes with significant errors in the estimation of the thermal conductivity values. Considering that Cu_2Se has been identified as a potential thermoelectric material,[11] it is necessary to understand the effect of temperature on its lattice thermal conductivity and the phonon thermal transport for usage in various

a)Electronic mail: jayantks@iitk.ac.in

industrial applications. Thus, the focus of this work is to understand the variation in the thermal conductivity of β-Cu_2Se and phonon thermal transport as a function of temperature using molecular dynamics (MD) simulations.

To perform the MD simulations, we have used the Morse potential derived by Namsani *et al.*[16] using DFT-based data, which was shown to reproduce the experimental structural and thermal properties of β-Cu_2Se. The Morse potential was also used successfully to model thermoelectric materials like Bi_2Te_3 and PbSe. The potential model used in this study is expressed in the following form:

$$E_{ij} = D\left[\left\{\left(1-\exp\left(-a(r_{ij}-r_0)\right)\right\}^2 - 1\right] + \frac{Cq_iq_j}{r_{ij}}, \quad (1)$$

where E_{ij} is the interaction energy of a pair of nonbonded atoms; i and j are atomic indexes and refer to either a Cu or a Se atom; D, a, r_0, and C are the model parameters; and q_i and q_j are the charges of the ions considered in this model.

Reverse non-equilibrium molecular dynamics[17] (RNEMD) simulations were used to compute the thermal conductivity. Figure 1 presents the system employed in the current work. In this approach, the simulation box was divided into 50 slabs (i.e., $N = 50$) along the heat transfer direction, where the first slab was assigned to the cold region and the 26th slab was assigned to the hot region. In other words, there were 24 intermediate slabs between the cold and hot regions. The kinetic energies of the coldest atoms in the cold slab and the hottest atoms in the hot slab were exchanged. This introduces heat flux in the system. Here, the heat flux was imposed on the β-Cu_2Se system along the z-direction. Using the kinetic energy exchanged in the system, heat flux in the z-direction (J_z) can be calculated using the following equation:

$$J_z = \frac{1}{2tA}\sum_{transfer}\frac{m}{2}\left(v_{hot}^2 - v_{cold}^2\right), \quad (2)$$

where m is the mass of the atoms, t is the time of simulations, A is the cross-sectional area of the simulation box, and v_{hot} and v_{cold} are the velocities of the selected atoms.

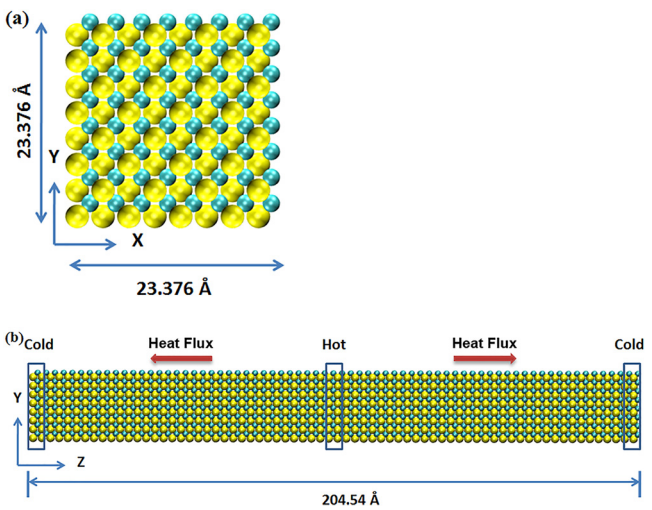

FIG. 1. (a) XY plane and (b) YZ plane of the β-Cu_2Se system considered in the simulations: yellow atoms are selenide (Se), and cyan atoms are copper (Cu).

Over the course of the simulation run, exchange of kinetic energy in the system induced a temperature gradient within the system. In this work, the flux rate is controlled by kinetic energy swapping between cold and hot slabs for every 0.2 ps and the flux rate that is obtained at 500 K is 1.803 eV/s. The temperature of each slab was computed using the equation given below. Further, the temperature profile was computed by averaging the temperature over a time interval of 100 ps

$$T_i(slab) = \frac{3}{2Nk_B}\sum_j \frac{p_j^2}{2m}. \quad (3)$$

Assuming the validity of a linear response (Fourier's law), the thermal conductivity of the system can be computed using the computed temperature gradient and the flux using the following equation:

$$k = \frac{-J_z}{\left\langle \frac{dT}{dz} \right\rangle}. \quad (4)$$

Here, k is the thermal conductivity, $\left\langle \frac{dT}{dz} \right\rangle$ is the temperature gradient, and J_z is the flux transferred within the Cu_2Se system.

Thermal conductivity calculations were performed over a temperature range of 400–1000 K using NPT (constant number of particles (N), pressure (P), and temperature (T)), NVT (constant N, volume (V) and T), and NVE (constant N, V and energy (E)) ensembles as implemented in the LAMMPS software.[18] First, we performed NPT ensemble simulations at a given temperature and a pressure of 1 atm for 4 ns. The final structure obtained from NPT simulations was used to perform NVT simulations of the system at a given temperature for 1 ns. The temperature and pressure of the system were maintained using a Nosé-Hoover thermostat and barostat.[19] These NPT and NVT simulations were performed using a time step of 0.5 fs. To compute the thermal conductivity of the Cu_2Se system at a particular temperature, the final structure from the NVT simulation was used to perform the NEMD simulation for 20 ns. All MD simulations were performed using the periodic boundary conditions in all the three directions.

In order to elucidate the effect of temperature on the thermal conductivity of Cu_2Se, we calculated the phonon density of states (DOS) from the Fourier transform of the velocity autocorrelation function (VACF)[20] at several temperatures. We performed 2 ns equilibration simulations of the system before applying the heat flux on Cu_2Se. Equilibrium simulations were then continued for 1 ns, and equilibrated structures were sampled every 100 ps. Each of these structures was again simulated for 10 ps, and velocities were sampled every 1 fs to calculate the VACF, obtained routinely from MD simulations.[21] The overall average of the VACF was Fourier transformed to obtain the phonon DOS at different temperatures. Using the equilibrium crystal structure, we have calculated the second order and third order forces using VASP along with PHONOPY and PHONO3PY,[22] which are interfaced with VASP to calculate the phonon DOS and lattice thermal conductivity within the framework of DFT. We

used the supercell approach to calculate the phonon DOS. In this study, we chose a supercell of $3 \times 3 \times 3$ containing 216 Cu atoms and 108 Se atoms to calculate the phonon DOS and lattice thermal conductivity. The forces were calculated at the equilibrium lattice constants using the PAW-PBE (Projector Augmented Wave - Perdew-Burke-Ernzerhof)[23] pseudopotential with an energy convergence of 10^{-8} eV. We checked the convergence of the phonon DOS with respect to the size of the supercells by performing calculations for different supercells.

RNEMD simulations were used to calculate the lattice thermal conductivity, as mentioned earlier. The length of the system was varied from 6 nm to 24 nm in the heat transport direction (z-direction) to study the effect of the system size on the thermal conductivity of β-Cu_2Se. The size-dependent thermal conductivity of the system is shown in Fig. 2(a). The thermal conductivity increases with increasing simulation system size for the temperature range considered in this study. However, the thermal conductivity decreases with increasing temperature. Figure 2(b) shows the variation in inverse thermal conductivity with an inverse system size at different temperatures. The inverse k data show a linear relationship with the inverse system size in the considered temperature range. The effective thermal conductivity of the system with an infinite size is computed by fitting the variation in the inverse thermal conductivity with the inverse of the simulation box length, as per the following equation:[24]

$$k_L^{-1} = k_\infty^{-1} + \left(\frac{12}{C_V v}\right) L^{-1}, \tag{5}$$

where, k_L, k_∞, C_v, v, and L are the length dependent thermal conductivity, thermal conductivity at the infinite length of the simulation system, volumetric specific heat, mean phonon velocity, and length of the simulation system, respectively. The above equation is fitted to the length dependent thermal conductivity data using RNEMD simulations to obtain the thermal conductivity value at the infinite length, which is shown in Fig. 2(c). The effective thermal conductivity decreases monotonically with increasing temperature. Further, the slope of the inverse thermal conductivity relation with the inverse of the length of the simulation system was used to compute the mean phonon velocity. The specific heat used was calculated via the vibrational partition function, and the corresponding equations are given below[25]

$$Z_{vib} = \sum_{k-points} w_k \sum_{all\ modes} \left(1 - \exp\left(-\frac{h\omega}{kT}\right)\right)^{-1}, \tag{6}$$

$$C_v = RT\left(2\left(\frac{\partial \ln Z_{vib}}{\partial T}\right) + T\left(\frac{\partial^2 \ln Z_{vib}}{\partial T}\right)\right). \tag{7}$$

The relationship between the thermal conductivity and the mean free path of phonons via the kinetic theory,[24] as shown below, was used to estimate the average mean free path of phonons

$$k = \frac{1}{3} C_V v_s l. \tag{8}$$

Here, k, C_V, v_s, and l are the thermal conductivity, volumetric specific heat, mean velocity of the sound, and average phonon mean free path. The C_v value and velocity of sound of the material were computed using GULP software.[25] Further, to gain additional insights into the phonon transport, we have computed the mean phonon lifetime, $\tau = l/v$. The obtained mean phonon velocities and lifetimes at different temperatures are presented in Table I.

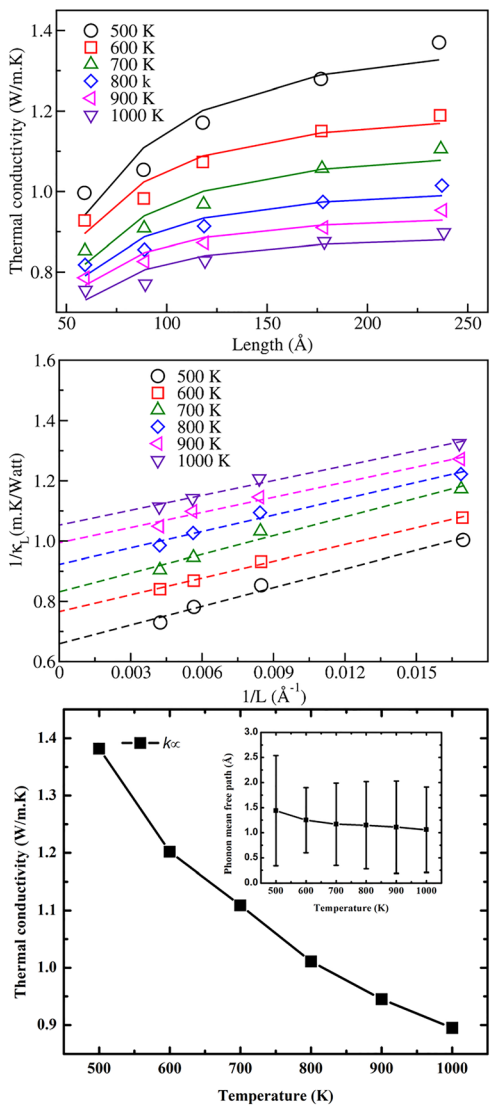

FIG. 2. (a) Thermal conductivity of β-Cu_2Se as a function of system size in the temperature range of 500–1000 K (solid lines are average trend lines). (b) Inverse thermal conductivity of β-Cu_2Se as a function of the inverse of the simulation system size. (c) The thermal conductivity at an infinite length of the simulation system size. The inset in this figure shows the change in the phonon mean free path as a function of temperature.

TABLE I. Calculated mean phonon velocities (v), average phonon mean free path (l), and mean phonon lifetimes at different temperatures. The deviations from the linearity of k and L data are used to compute the uncertainties in the simulation data and presented along with the values.

T (K)	v (km/s)	l (Å)	τ (ps)
500	2.44 ± 1.78	1.44 ± 1.10	0.59 ± 0.62
600	2.74 ± 0.85	1.25 ± 0.65	0.46 ± 0.27
700	2.48 ± 1.25	1.17 ± 0.82	0.47 ± 0.40
800	3.03 ± 2.13	1.15 ± 1.52	0.38 ± 0.56
900	4.23 ± 1.33	1.11 ± 0.92	0.26 ± 0.23
1000	7.51 ± 0.76	1.06 ± 0.85	0.14 ± 0.11

The change in the average phonon mean free path is around 26% with the increase in the temperature from 500 K to 1000 K. In contrast, phonon velocity on average increases by 200%, and correspondingly, the phonon lifetime decreases by 76% upon increasing the temperature from 500 K and 100 K. Clearly, phonon velocity is most sensitive to the change in the temperature. The computed average phonon mean free path and phonon lifetime decrease with the increase in temperature. It is observed that the increase in temperature increases the atomic diffusion of Cu within the Se framework of β-Cu_2Se, causing enhancement in the phonon scattering, and subsequently decreases the phonon lifetime. The computed mean free path of phonons in the system at different temperatures is shown as an inset in Fig. 2(c). The obtained average phonon mean free path is between 1.44 and 1.06 Å in the temperature range of 500–1000 K. The average phonon mean free path for β-Cu_2Se is slightly lower than the values reported for other thermoelectric materials such as $CoSb_3$ (Ref. 26), $Ba_8Ga_{16}Ge_{30}$ (Ref. 4) (4–5 Å), Bi_2Te_3 (Ref. 27), and In_4Se_3 (Ref. 28) (~2 Å).

Figure 3 shows a comparison of the computed effective κ_L values of β-Cu_2Se over a temperature range of 400–1000 K from various previously reported values[6,8,15] as well as the calculated κ_L values from the current work. In recent years, various attempts were made by experimental groups to estimate the lattice thermal conductivity of β-Cu_2Se, using similar methodologies. However, the results reported are not in good agreement as clearly evident from Fig. 3. It is observed by Liu *et al.*[6] that low copper deficiency can significantly affect the thermal conductivity values. Further, experimental work yields the total thermal conductivity, which is the sum of electronic thermal conductivity and lattice thermal conductivity. The electronic thermal conductivity is calculated by $\kappa_e = L_0\sigma T$, where L_0 is the Lorenz number, σ is the electrical conductivity, and T is the absolute temperature. The κ_L value of a material is estimated by simply subtracting κ_e from its total thermal conductivity. The Lorenz numbers used in the calculation of electronic thermal conductivity in experiments vary in the range of 1.5×10^{-8} to $2.0 \times 10^{-8}\,V^{-2}K^{-2}$. Thus, systematic errors in the calculation of thermal conductivity and small variation in the copper concentration may possibly be the reasons for the variation in the experimental data reported in Fig. 3. Considering the significant variation in the experimental data, the thermal conductivity values from the RNEMD simulations are reasonable. It is also noted that the change in the thermal conductivity per degree change in temperature (i.e., $\Delta\kappa_L/\Delta T$, the slope of the thermal conductivity profile) depends on the copper concentration as reported by Liu *et al.*[6] In this work, the slope, $\Delta\kappa_L/\Delta T$, is in very good agreement with the data reported by Kim *et al.*[15] It is also noted that the thermal conductivity values due to the RNEMD simulations are closest to those due to experimental values in the study by Gahtori *et al.*[8] in the temperature range of 500–800 K. Figure 3 also includes the thermal conductivity values obtained from the DFT calculations. The values are relatively lower, particularly at higher temperature, compared to those obtained from the experiments and RNEMD simulations. This is attributed to the approximations and the system size considered in the DFT calculations.

To understand the change in the mechanism of heat transfer and thermal conductivity with temperature, we computed phonon DOS using the Fourier transform of the VACF obtained from MD simulations. The calculated phonon DOS at various temperatures is shown in Fig. 4.

We observed three vibrational modes in phonon DOS for all the temperatures: two modes are at low frequencies and one is at a high frequency. The highest frequency phonon mode at 500 K is at 275 cm^{-1} (P3). This is in good agreement with the Raman mode observed for Cu_2Se[29] at 262 cm^{-1}. This mode of frequency is attributed to the Se-Se vibrational mode in the system.[30] The two low-frequency modes, at 107 cm^{-1} (P2) and 60 cm^{-1} (P1), are in good agreement with the vibrational modes observed experimentally between 105 and 108 cm^{-1} and between 60 and 70 cm^{-1} in the Raman and IR spectra, respectively.[31] There is a shift in the phonon modes toward lower frequencies with increasing temperature. This shift is clearly illustrated by the vertical dotted lines in Fig. 4, which represent the three phonon modes at 500 K. The shift and broadening of the peak toward lower frequencies imply that the increase in temperature reduces the heat-carrying capacity of Cu_2Se, as also observed in experiments.[6] This reduced heat-carrying capacity logically results in lower thermal conductivity values of Cu_2Se at higher temperatures. The phonon modes shift towards the lower frequency, which is more pronounced at temperatures higher than its glass temperature (800 K) primarily because of increased diffusion of Cu atoms at higher temperatures.[15,16] The observation is also in line with the experimental work of Liu *et al.*[6] The increased diffusion of Cu atoms within the framework of Se

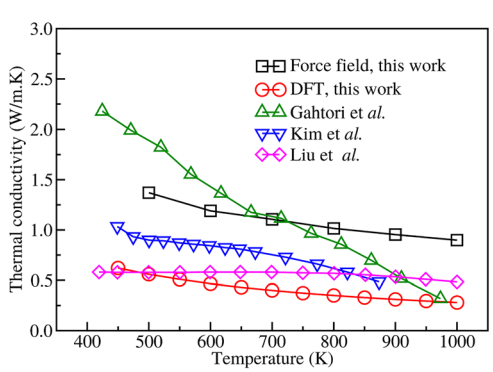

FIG. 3. Comparison of thermal conductivity values computed using RNEMD simulations and DFT with the available experimental data.

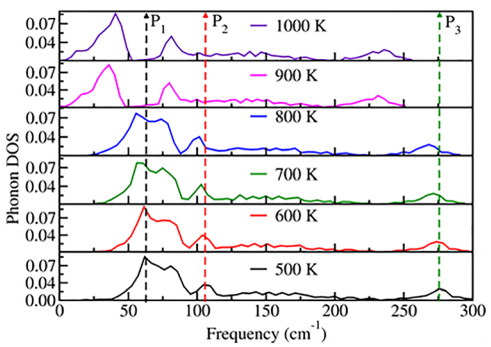

FIG. 4. Phonon DOS computed in the temperature range of 500–1000 K. The dotted lines represent the frequencies corresponding to the dominant phonon modes (P1, P2, and P3) observed at 500 K.

atoms results in phonon scattering, as discussed earlier, and shifting of phonon modes to lower frequencies. These are primarily reasons behind the reduction in the thermal conductivity of β-Cu_2Se with increasing temperature.

In summary, the RNEMD simulation was used to calculate the thermal conductivity values of β-Cu_2Se in the temperature range of 400–1000 K. The computed thermal conductivity values are in reasonable agreement within the range of previously reported experimental results. The length-dependent thermal conductivity is successfully used to predict the phonon mean free path in the considered temperature range. The average phonon mean free path is found to decrease with increasing temperature, with values between 1.0 and 1.5 Å in the temperature range of 500–1000 K. The decreasing thermal conductivity with increasing temperature is due to the shift of phonon modes toward lower frequencies with increasing temperature, which is explained through phonon DOS calculations. The dominant phonon modes observed in phonon DOS are in good agreement with the vibrational modes in the Raman and IR spectra observed using experiments.

The High Performance Computing (HPC) facility of the Indian Institute of Technology, Kanpur, is gratefully acknowledged. S.A. would like to acknowledge the use of the computing facilities at the Intra University Accelerator Centre in New Delhi, Institute of Mathematical Sciences in Chennai, and CSIR-Fourth Paradigm Institute in Bengaluru.

[1]D. M. Rowe, *Thermoelectrics Handbook: Macro to Nano* (CRC Press, 2010).
[2]W. Liu, X. Yan, G. Chen, and Z. Ren, Nano Energy **1**(1), 42 (2012).
[3]B. C. Sales, D. Mandrus, and R. K. Williams, Science **272**(5266), 1325 (1996).
[4]M. Christensen, A. B. Abrahamsen, N. B. Christensen, F. Juranyi, N. H. Andersen, K. Lefmann, J. Andreasson, C. R. H. Bahl, and B. B. Iversen, Nat. Mater. **7**(10), 811 (2008).
[5]B. Poudel, Q. Hao, Y. Ma, Y. Lan, A. Minnich, B. Yu, X. Yan, D. Wang, A. Muto, D. Vashaee, X. Chen, J. Liu, M. S. Dresselhaus, G. Chen, and Z. Ren, Science **320**(5876), 634 (2008); K. F. Hsu, S. Loo, F. Guo, W. Chen, J. S. Dyck, C. Uher, T. Hogan, E. K. Polychroniadis, and M. G. Kanatzidis, *ibid.* **303**(5659), 818 (2004).
[6]H. Liu, X. Shi, F. Xu, L. Zhang, W. Zhang, L. Chen, Q. Li, C. Uher, T. Day, and G. J. Snyder, Nat. Mater. **11**(5), 422 (2012).
[7]M. C. Nguyen, J.-H. Choi, X. Zhao, C.-Z. Wang, Z. Zhang, and K.-M. Ho, Phys. Rev. Lett. **111**(16), 165502 (2013); X.-X. Xiao, W.-J. Xie, X.-F. Tang, and Q.-J. Zhang, Chin. Phys. B **20**(8), 087201 (2011); B. Yu, W. Liu, S. Chen, H. Wang, H. Wang, G. Chen, and Z. Ren, Nano Energy **1**(3), 472 (2012); S. Bhattacharya, R. Basu, R. Bhatt, S. Pitale, A. Singh, D. K. Aswal, S. K. Gupta, M. Navaneethan, and Y. Hayakawa, J. Mater. Chem. A **1**(37), 11289 (2013); S. Ballikaya, H. Chi, J. R. Salvador, and C. Uher, *ibid.* **1**(40), 12478 (2013).
[8]B. Gahtori, S. Bathula, K. Tyagi, M. Jayasimhadri, A. K. Srivastava, S. Singh, R. C. Budhani, and A. Dhar, Nano Energy **13**, 36 (2015).
[9]M. Råsander, L. Bergqvist, and A. Delin, J. Phys.: Condens. Matter **25**(12), 125503 (2013).
[10]Y. Zhang, Y. Wang, L. Xi, R. Qiu, X. Shi, P. Zhang, and W. Zhang, J. Chem. Phys. **140**(7), 074702 (2014).
[11]K. Tyagi, B. Gahtori, S. Bathula, S. Auluck, and A. Dhar, Appl. Phys. Lett. **105**(17), 173905 (2014).
[12]L. D. Hicks and M. S. Dresselhaus, Phys. Rev. B **47**(19), 12727 (1993); Y. Pei, X. Shi, A. LaLonde, H. Wang, L. Chen, and G. J. Snyder, Nature **473**(7345), 66 (2011); K. Biswas, J. He, I. D. Blum, C.-I. Wu, T. P. Hogan, D. N. Seidman, V. P. Dravid, and M. G. Kanatzidis, Nature **489**(7416), 414 (2012).
[13]X. Zhang and L.-D. Zhao, J. Materiomics **1**, 92 (2015).
[14]B.-L. Huang and M. Kaviany, Phys. Rev. B **77**(12), 125209 (2008); X. Cartoixà, R. Dettori, C. Melis, L. Colombo, and R. Rurali, Appl. Phys. Lett. **109**(1), 013107 (2016); W. J. Evans, L. Hu, and P. Keblinski, *ibid.* **96**(20), 203112 (2010); F. Leroy, J. Schulte, G. Balasubramanian, and M. C. Böhm, J. Chem. Phys. **140**(14), 144704 (2014).
[15]H. Kim, S. Ballikaya, H. Chi, J.-P. Ahn, K. Ahn, C. Uher, and M. Kaviany, Acta Mater. **86**, 247 (2015).
[16]S. Namsani, B. Gahtori, S. Auluck, and J. K. Singh, J. Comput. Chem. **38**(25), 2161 (2017).
[17]M.-P. Florian, J. Chem. Phys. **106**(14), 6082 (1997).
[18]S. Plimpton, J. Comput. Phys. **117**(1), 1 (1995).
[19]S. Nose, J. Chem. Phys. **81**(1), 511 (1984).
[20]M. T. Dove, *Introduction to Lattice Dynamics* (Cambridge University Press, Cambridge, 1993).
[21]M. P. Allen and D. J. Tildesley, *Computer Simulation of Liquids* (Oxford University Press, New York, 1987).
[22]A. Togo and I. Tanaka, Scr. Mater. **108**, 1 (2015); G. Kresse and J. Hafner, Phys. Rev. B **47**(1), 558 (1993); J. Hafner, G. Kresse, and J. Hafner, *ibid.* **49**(20), 14251 (1994).
[23]G. Kresse and J. Hafner, J. Phys.: Condens. Matter **6**(40), 8245 (1994).
[24]S. Stackhouse, L. Stixrude, and B. B. Karki, Phys. Rev. Lett. **104**(20), 208501 (2010).
[25]J. D. Gale, J. Chem. Soc., Faraday Trans. **93**(4), 629 (1997); J. D. Gale and A. L. Rohl, Mol. Simul. **29**(5), 291 (2003).
[26]T. Caillat, A. Borshchevsky, and J.-P. Fleurial, J. Appl. Phys. **80**(8), 4442 (1996).
[27]B. Y. Yavorsky, N. F. Hinsche, I. Mertig, and P. Zahn, Phys. Rev. B **84**(16), 165208 (2011).
[28]J.-S. Rhyee, E. Cho, K. H. Lee, S. M. Lee, S. Il Kim, H.-S. Kim, Y. S. Kwon, and S. J. Kim, Appl. Phys. Lett. **95**(21), 212106 (2009).
[29]B. Minceva-Sukarova, M. Najdoski, I. Grozdanov, and C. J. Chunnilall, J. Mol. Struct. **410**, 267 (1997).
[30]C. Xue, D. Papadimitriou, Y. S. Raptis, W. Richter, N. Esser, S. Siebentritt, and M. C. Lux-Steiner, J. Appl. Phys. **96**(4), 1963 (2004); V. Lesnyak, R. Brescia, G. C. Messina, and L. Manna, J. Am. Chem. Soc. **137**(29), 9315 (2015).
[31]M. Gilić, M. Petrović, R. Kostić, D. Stojanović, T. Barudžija, M. Mitrić, N. Romčević, U. Ralević, J. Trajić, M. Romčević, and I. S. Yahia, Infrared Phys. Technol. **76**, 276 (2016); A. N. Tiwari, S. Blunier, M. Filzmoser, H. Zogg, D. Schmid, and H. W. Schock, Appl. Phys. Lett. **65**(26), 3347 (1994); C. Rincón and F. J. Ramírez, J. Appl. Phys. **72**(9), 4321 (1992).